Hemispheric asymmetry of the afternoon electron aurora

M. O. Fillingim, G. K. Parks, H. U. Frey, T. J. Immel, and S. B. Mende
Space Sciences Laboratory, University of California, Berkeley, California, USA

Received 29 September 2004; revised 30 December 2004; accepted 18 January 2005; published 11 February 2005.

[1] Using ultraviolet images from two global auroral imagers, IMAGE FUV in the northern hemisphere and Polar UVI in the south, we present the first synoptic scale conjugate observations of the dayside aurora. We find that the morphology of the afternoon aurora is significantly different in the two hemispheres. Multiple spots in a "string of pearls" configuration are seen in the southern hemisphere while the northern aurora is unstructured. We relate the observed asymmetry in the aurora to the Y GSM component of the IMF: a strong IMF B_Y modifies the ionospheric convection and field aligned current patterns, leading to the auroral asymmetry. Additionally, we suggest that the instability giving rise to the multiple spot morphology occurs at low altitude. **Citation:** Fillingim, M. O., G. K. Parks, H. U. Frey, T. J. Immel, and S. B. Mende (2005), Hemispheric asymmetry of the afternoon electron aurora, *Geophys. Res. Lett.*, *32*, L03113, doi:10.1029/2004GL021635.

1. Introduction

[2] A region of persistent auroral emission centered in the afternoon sector (~15 MLT) near 75° magnetic latitude has been observed since the earliest days of spaceborne auroral imagers [*Cogger et al.*, 1977]. These early results were later substantiated by auroral observations by Viking [*Lui et al.*, 1987] and Polar [*Liou et al.*, 1997]. The imaging results have been corroborated by in-situ measurements of the source particles. Particle data from ISIS-2 [*McDiarmid et al.*, 1975], TIROS-N [*Evans*, 1985], and DMSP [*Newell et al.*, 1996] have all shown a maximum in the <~1 keV electron precipitation near 15 MLT and 75° magnetic latitude. This region of increased auroral brightness and particle precipitation is co-located with a statistical maximum in the Region 1 upward field aligned current as reported by *Iijima and Potemra* [1978]. Therefore, a consistent picture has developed with the afternoon bright spot interpreted as the auroral signature of the maximum in the Region 1 current which is carried by precipitating electrons [*Potemra et al.*, 1990; *Liou et al.*, 1999].

[3] Though persistent in a statistical sense, the presence of the afternoon auroral emission is influenced by solar wind parameters. *Murphree et al.* [1981] and *Vo and Murphree* [1995] found that afternoon auroral bright spots in the northern hemisphere are more common when the IMF B_Y component is negative. Also, spots are more likely to be present during times of high solar wind speed (>~500 km/s) and low density (<~7 cm^{-3}).

[4] *Lui et al.* [1987] was the first to report multiple spots aligned in a "string of pearls" configuration. Additional work by *Lui et al.* [1989], *Potemra et al.* [1990], *Rostoker et al.* [1992], and *Vo and Murphree* [1995] showed that the occurrence of one to four spots simultaneously is common, the spots have spatial sizes between 50 and 200 km in the ionosphere, separations between spots are about 1 hour of local time (~500 km), and individual spots are transient, typically lasting only 1 to 10 minutes. These authors suggested that a Kelvin-Helmholtz (K-H) instability in the low latitude boundary layer could be a possible generation mechanism for multiple auroral spots in the afternoon sector.

[5] A statistical survey of global auroral images by *Liou et al.* [2001] revealed that auroral emission in the afternoon sector is enhanced in the summer (under sunlit conditions) and suppressed in the winter (in darkness). The opposite was observed on the nightside. Directly comparing auroral brightness with solar EUV conductance, *Shue et al.* [2001] reported that the auroral brightness-conductance relationship in the afternoon region is more complex than that observed at other local times. For small conductance, increases in the conductance enhance the auroral brightness, as is common on the dayside. However, higher levels of conductance reduce the auroral luminosity, as is typical of the nightside. These variations with season/conductance, while statistical, suggest that there may be hemispheric differences in the presence and behavior of the 15 MLT bright spot.

[6] The previous work on the conjugacy of dayside aurora can be divided into two categories: comparison of optical data in one hemisphere with non-optical data (magnetometer or in situ particle data) from the conjugate hemisphere [*Dickinson et al.*, 1986; *Mende et al.*, 1990; *Vo et al.*, 1995] and comparison of optical data from both hemispheres [*Burns et al.*, 1990, 1992]. *Dickinson et al.* [1986] were the first to investigate the conjugacy of dayside auroral features. By comparing low altitude satellite particle data from the northern hemisphere to ground based all sky images at South Pole, they found a shift in latitude between the maximum auroral precipitation with the northern hemisphere emissions being located further poleward in the afternoon sector. Their technique was only sensitive to shifts in latitude; they were unable to address temporal or longitudinal conjugacy. *Mende et al.* [1990], by using ground magnetometer data in the northern hemisphere and all sky camera images from South Pole during five dayside magnetic impulse events, found good agreement between the timing of magnetic bays and brightenings of the aurora. It was impossible, however, to determine spatial conjugacy. Viking images from the northern hemisphere and DMSP particle precipitation data in the southern hemisphere were used by *Vo et al.* [1995] to examine the latitudinal conjugacy of the dayside aurora. In agreement with *Dickinson et al.* [1986], they found that the northern aurora was shifted ~4° poleward of the expected conjugate point in the afternoon sector.

0094-8276/05/2004GL021635$05.00

[7] The only optical-optical studies of the conjugacy of the afternoon aurora have been done by *Burns et al.* [1990, 1992]. They compared Viking images from the northern hemisphere to ground based keogram and all sky camera data from South Pole. They were able to determine a shift in latitude (northern aurora about 4° poleward) and local time (1 hour later) of the observed conjugate points with respect to the IGRF model predictions. The width and motion of the auroral forms in the opposite hemispheres could differ significantly at times. They also noted short lived features observed in the southern hemisphere but not in the north which they suggested could be accounted for by local acceleration processes.

[8] All of these previous conjugate studies have been limited to small scale features by relying on either in-situ point measurements or ground based instruments in at least one hemisphere. To date, there have been no comparisons of global images from conjugate hemispheres on the dayside. Between October 2002 and March 2003, global auroral imagers on the IMAGE and Polar spacecraft were in the unique position to view the dayside aurora in the northern and southern hemispheres simultaneously. With these data, we are able to address the issue of conjugacy of the dayside aurora on a synoptic scale for the first time. In this Letter, we highlight one example displaying clear morphological asymmetry and discuss possible mechanisms that may lead to the observed asymmetry.

2. Instrumentation

[9] The images of the northern aurora are taken by the Wideband Imaging Camera (WIC), part of the Far Ultraviolet (FUV) suite of instruments on the IMAGE spacecraft [*Mende et al.*, 2000]. WIC is sensitive to Lyman-Birge-Hopfield (LBH) emissions from 1400 to 1900 Å.

[10] Southern hemisphere auroral images are obtained by the Ultraviolet Imager (UVI) onboard the Polar spacecraft [*Torr et al.*, 1995]. UVI is equipped with four narrow band UV filters. Images taken with the two filters sensitive to LBH emissions are shown. The filter which passes the shorter wavelengths of the LBH emissions (LBHS) has a bandwidth of ~200 Å centered at 1500 Å. The filter which passes the longer wavelengths (LBHL) has a similar bandwidth and is centered at 1700 Å. Both the UVI LBHS and LBHL filters are contained within the WIC bandpass. Also, the peak response of WIC coincides with the LBHS filter.

[11] The integration time of WIC is 10 seconds, and one image is obtained every 2 minutes. UVI has multiple modes of operation. For the event shown here, the instrument is alternating 18 and 37 second integration times while cycling through different filters. The time between images with the same integration period with the same filter is about 5 minutes.

[12] Despite orbit and detector differences, the spatial resolution of WIC and UVI are comparable. The spatial resolution of WIC at apogee is 50 km; for UVI, it is 30 km.

3. Morphological Asymmetry

[13] At 19 UT on 4 November 2002, IMAGE was located in the northern hemisphere at [3.9, −4.3, 5.4] R_E GSE, and FUV was observing the dayside northern aurora. Polar was located at [−2.7, 5.8, −3.2] R_E GSE, and UVI was observing the duskside southern aurora.

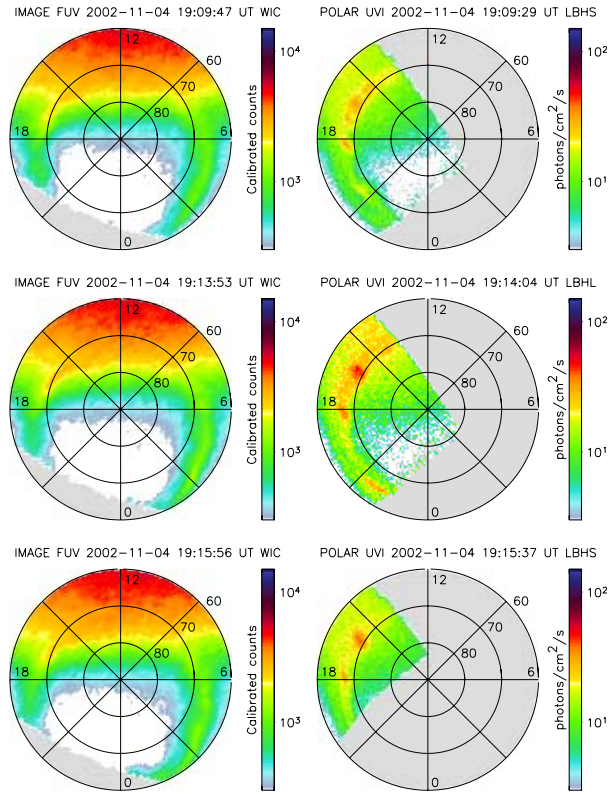

Figure 1. Left: images of the northern aurora from IMAGE FUV WIC; right: images of the southern aurora (as viewed looking through Earth) from Polar UVI. The gray shaded regions are outside the imagers' fields of view.

[14] Figure 1 (left) shows the northern aurora as viewed by WIC projected into Magnetic Apex Coordinates [*VanZandt et al.*, 1972; *Richmond*, 1995]. Local noon is toward the top and dusk is toward the left. The beginning of each 10 second image integration time is shown at the top. There are four minutes between the first and second image, and the nominal two minutes between the second and third. A line-of-sight correction, compensates for the increased emission due to the longer path length through the atmosphere for slant viewing as compared to nadir viewing, has been applied to these images. The large region of bright emission at the top of each image is dayglow due to scattered sunlight.

[15] In all three images there is an enhancement in the auroral intensity in the afternoon sector. The enhanced emission extends only a few degrees in latitude and from 15 MLT to near 18 MLT. Note the lack of distinct structure in this region in all three images.

[16] The UVI images from the southern hemisphere whose integration times are closest to those of the WIC images are shown in Figure 1 (right). The image projection is such that the observer is looking through Earth from above the north pole so that the coordinate system is the same as in the left column. The first and third images are taken with the LBHS filter and have integration times of 37 seconds. The second image is taken with the LBHL filter

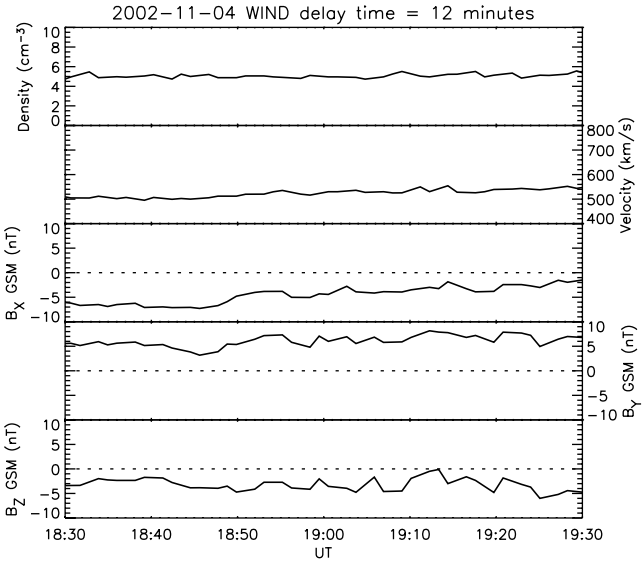

Figure 2. Solar wind and IMF data from the Wind spacecraft propagated to Earth.

and has an integration time of 18 seconds. These images have also been line-of-sight corrected.

[17] Several dim spots in the region from 15 to 18 MLT are seen in the first image. These spots are a few hundred km in size in the ionosphere and are similar to those shown by *Lui et al.* [1987, 1989], *Potemra et al.* [1990], and *Rostoker et al.* [1992]. (The Polar spacecraft "wobble" is approximately in the 03−15 MLT direction at this time. The latitudinal extent of the spots is overestimated, but the width of the spots in local time is unaffected.) Four minutes later, in the second image, one bright spot remains near 16 MLT and a dimmer spot is seen at 18 MLT. The same two spots are still seen 2 minutes later. The spot near 16 MLT is much brighter than any of the spots in the first image taken with the same filter. Note that the same features are seen in the second and third UVI images taken with two different LBH filters. Both filters are within the WIC bandpass, but no similar features are seen in the northern hemisphere. The southern dayside aurora is structured and dynamic while the northern aurora is unstructured and static.

[18] The solar wind parameters observed by Wind near the time of these images are plotted in Figure 2. Wind was located at [60, −28, 5] R_E GSE. The data have been shifted by 12 minutes to account for the travel time from Wind to Earth. The IMF data are in GSM coordinates. The solar wind conditions are relatively steady throughout the interval. The solar wind density is nearly constant at about 5 cm^{-3}. The solar wind velocity averages about 500 km/s. The IMF $B_X \sim -5$ nT, and $B_Y \sim 5$ nT with minor variations. B_Z is negative and on the order of a few nT.

4. Discussion

[19] There are several possible explanations for the observed asymmetry in the afternoon aurora. One is that the source population does not have access to both points in the ionosphere; i.e., the two points are not in fact conjugate. The field lines which have their footprints at the bright spots may be open. This idea can explain how auroral structure can occur in one hemisphere and not simultaneously in the other, although magnetic field models do not support this conjecture.

[20] Alternatively, local acceleration processes could account for the observed asymmetry. *Newell et al.* [1996] have shown that although the accelerating potentials are small ($<\sim$1 keV), local mechanisms are accelerating the precipitating particles in this region. *Burns et al.* [1992] also invoked local acceleration processes to account for differences seen in the aurora in opposite hemispheres.

[21] The underlying cause of the asymmetry in local acceleration processes is unknown. Seasonal differences in the auroral behavior may be related to differences in ionospheric conductivity [*Liou et al.*, 2001; *Shue et al.*, 2001]. The dipole tilt angle for this event is −7°, so the southern hemisphere experiences slightly more direct illumination. The solar zenith angle (SZA) for the northern hemisphere emission is between 90 and 95°. The spots in the southern hemisphere near 16 MLT and 18 MLT have SZAs of 75° and 85°, respectively. Since the tilt angle and differences in the SZAs are small, it is expected that differences in ionospheric conductivity play a relatively minor role.

[22] The large scale morphological asymmetry can be explained in part by the solar wind-magnetosphere interaction when the IMF B_Y component is significant. The ionospheric convection patterns in the northern and southern hemispheres are mirror images of each other when the IMF has a B_Y component [e.g., *Heppner and Maynard*, 1987]. When B_Y is positive, as it is in this case, there is a circular convection cell on the duskside and a crescent-shaped cell on the dawnside in the northern hemisphere. In the southern hemisphere, a crescent-shaped cell is on the duskside and a circular cell is at dawn. A strong flow shear is present in the crescent-shaped cell which leads to a large divergence of ionospheric electric field and perpendicular current; hence a strong field aligned current (FAC) is present. This FAC flows downward into the ionosphere in the dawnside and upward at dusk. These are the Region 1 currents. Therefore, when a significant IMF B_Y is present, an asymmetry in the Region 1 current intensity and distribution is expected on the duskside. When B_Y is positive (this case), there should be a stronger upward FAC on the duskside in the southern hemisphere; for B_Y negative, the FAC should be more intense in the north [cf. *Kozlovsky et al.*, 2003]. Since the upward current is carried by downward electrons, we can predict a similar asymmetry in the afternoon aurora. This is similar to the prediction made by *Robinson et al.* [1986] regarding the IMF B_Y control of dayside precipitation in the northern hemisphere. We have extended this to predict an asymmetry between the northern and southern duskside aurora.

[23] The presence of multiple spots in a "string of pearls" configuration has been interpreted as a result of a K-H type instability at the flank magnetopause [*Lui et al.*, 1989; *Rostoker et al.*, 1992; *Wei and Lee*, 1993]. If this were the case, one may expect to see multiple spots in both hemispheres, not just in one. Presumably, if the instability occurs at the equator, the disturbance would propagate down the field line to the conjugate ionospheres. These observations are not consistent with such a picture.

[24] A new interpretation is that the instability develops in the ionosphere at low altitudes rather than at the equator.

Ridley and Clauer [1996] observed a K-H type instability at the convection reversal boundary when $|B_Y/B_Z|$ in the IMF became larger than ~1.5. These oscillations of the convection reversal boundary may be related to the multiple auroral spots seen in the afternoon sector. The instability mechanism responsible for their observations appears to be governed by the IMF orientation rather than the solar wind velocity, contrary to what is expected for a K-H instability occurring at the flank magnetopause.

5. Conclusion

[25] We have shown the first global scale conjugate observations of the dayside aurora. The observations show that there can be a morphological difference in the afternoon aurora in the two hemispheres. We propose that the asymmetry is due to a significant Y component of the IMF. The IMF modifies the ionospheric convection pattern and leads to a hemispheric asymmetry in the Region 1 FAC. Based on this, a prediction is made: the afternoon aurora should be brighter and more structured in the southern hemisphere when B_Y is positive and in the north when B_Y is negative. This prediction applies when B_Z is negative, as it is in this case. In contrast with previous suggestions, we also propose that the instability that gives rise to multiple spots in a ''string of pearls'' configuration occurs at low altitude near the ionosphere rather than at the equatorial flank magnetopause.

[26] We will continue to analyze conjugate images of the dayside aurora to test our predictions. Additionally, other ionospheric data (e.g., current densities and distributions, ionospheric electric fields, and convection patterns) will be compared to the images to determine if our proposed mechanism is viable.

[27] **Acknowledgments.** The Wind magnetometer (MFI) data are courtesy of R. L. Lepping. The Wind particle (3DP) data are courtesy of R. P. Lin. This work was supported by NASA grant NAG5-11416.

References

Burns, G. B., D. J. McEwen, R. A. Eather, F. T. Berkey, and J. S. Murphree (1990), Optical auroral conjugacy: Viking UV images—South pole station ground data, *J. Geophys. Res.*, *95*(A5), 5781–5790.

Burns, G. B., D. J. McEwen, F. T. Berkey, J. S. Murphree, D. Hearn, and R. A. Eather (1992), Dynamics of the conjugate post-noon regions during an auroral enhancement, *J. Geomag. Geoelectr.*, *44*(2), 65–90.

Cogger, L. L., J. S. Murphree, S. Ismail, and C. D. Anger (1977), Charactersitics of dayside 5577 Å and 3914 Å aurora, *Geophys. Res. Lett.*, *4*(10), 413–416.

Dickinson, D. F., S. B. Mende, and D. S. Evans (1986), Dayside variation in auroral conjugacy, *Geophys. Res. Lett.*, *13*(1), 68–71.

Evans, D. S. (1985), The characteristics of a persistent auroral arc at high latitude in the 1400 MLT sector, in *The Polar Cusp*, edited by J. A. Holtet and A. Egeland, pp. 99–109, Springer, New York.

Heppner, J. P., and N. C. Maynard (1987), Empirical high-latitude electric field models, *J. Geophys. Res.*, *92*(A5), 4467–4489.

Iijima, T., and T. A. Potemra (1978), Large-scale characteristics of field-aligned currents associated with substorms, *J. Geophys. Res.*, *83*(A2), 599–615.

Kozlovsky, A., T. Turunen, A. Koustov, and G. Parks (2003), IMF By effects in the magnetospheric convection on closed magnetic field lines, *Geophys. Res. Lett.*, *30*(24), 2261, doi:10.1029/2003GL018457.

Liou, K., P. T. Newell, C.-I. Meng, M. Brittnacher, and G. Parks (1997), Synoptic auroral distribution: A survey using Polar ultraviolet imagery, *J. Geophys. Res.*, *102*(A12), 27,197–27,205.

Liou, K., P. T. Newell, C.-I. Meng, T. Sotirelis, M. Brittnacher, and G. Parks (1999), Source region of 1500 MLT auroral bright spots: Simultaneous Polar UV images and DMSP particle data, *J. Geophys. Res.*, *104*(A11), 24,587–24,602.

Liou, K., P. T. Newell, and C.-I. Meng (2001), Seasonal effects on auroral particle acceleration and precipitation, *J. Geophys. Res.*, *106*(A4), 5531–5542.

Lui, A. T. Y., D. Venkatesan, G. Rostoker, J. S. Murphree, C. D. Anger, L. L. Cogger, and T. A. Potemra (1987), Dayside auroral intensifications during an auroral substorm, *Geophys. Res. Lett.*, *14*(4), 415–418.

Lui, A. T. Y., D. Venkatesan, and J. S. Murphree (1989), Auroral bright spots on the dayside oval, *J. Geophys. Res.*, *94*(A5), 5515–5522.

McDiarmid, I. B., J. R. Burrows, and E. E. Budzinski (1975), Average characteristics of magnetospheric electrons (150 eV to 200 keV) at 1400 km, *J. Geophys. Res.*, *80*(1), 73–79.

Mende, S. B., R. L. Rairden, L. J. Lanzerotti, and C. G. Maclennan (1990), Magnetic impulses and associated optical signatures in the dayside aurora, *Geophys. Res. Lett.*, *17*(2), 131–134.

Mende, S. B., et al. (2000), Far ultraviolet imaging from the IMAGE spacecraft. 2. Wideband FUV imaging, *Space Sci. Rev.*, *91*(1–2), 271–285.

Murphree, J. S., L. L. Cogger, and C. D. Anger (1981), Characteristics of the instantaneous auroral oval in the 1200–1800 MLT sector, *J. Geophys. Res.*, *86*(A9), 7657–7668.

Newell, P. T., K. M. Lyons, and C.-I. Meng (1996), A large survey of electron acceleration events, *J. Geophys. Res.*, *101*(A2), 2599–2614.

Potemra, T. A., H. Vo, D. Venkatesan, L. L. Cogger, R. E. Erlandson, L. J. Zanetti, P. F. Bythrow, and B. J. Anderson (1990), Periodic auroral forms and geomagnetic field oscillations in the 1400 MLT region, *J. Geophys. Res.*, *95*(A5), 5835–5844.

Richmond, A. D. (1995), Ionospheric electrodynamics using magnetic apex coordinates, *J. Geomag. Geoelectr.*, *47*(2), 191–212.

Ridley, A. J., and C. R. Clauer (1996), Characterization of the dynamic variations of the dayside high-latitude ionospheric convection reversal boundary and relationship to interplanetary magnetic field orientation, *J. Geophys. Res.*, *101*(A5), 10,919–10,938.

Robinson, R. M., C. R. Clauer, O. de la Beaujardiere, J. D. Kelly, and D. S. Evans (1986), IMF B_y control of ionization and electric fields measured by the Sondestrom radar, in *Solar Wind-Magnetosphere Coupling*, edited by Y. Kamide and J. A. Slavin, pp. 507–518, Terra Sci., Tokyo.

Rostoker, G., B. Jackel, and R. L. Arnoldy (1992), The relationship of periodic structures in auroral luminosity in the afternoon sector of ULF pulsations, *Geophys. Res. Lett.*, *19*(6), 613–616.

Shue, J.-H., P. T. Newell, K. Liou, and C.-I. Meng (2001), The quantitative relationship between auroral brightness and solar EUV Pedersen conductance, *J. Geophys. Res.*, *106*(A4), 5883–5894.

Torr, M. R., et al. (1995), A far ultraviolet imager for the International Solar-Terrestrial Physics mission, *Space Sci. Rev.*, *71*(1–4), 329–383.

VanZandt, T. E., W. L. Clark, and J. M. Warnock (1972), Magnetic apex coordinates: A magnetic coordinate system for the ionospheric F_2 layer, *J. Geophys. Res.*, *77*(13), 2406–2411.

Vo, H. B., and J. S. Murphree (1995), A study of dayside auroral bright spots seen by the Viking auroral imager, *J. Geophys. Res.*, *100*(A3), 3649–3655.

Vo, H. B., J. S. Murphree, D. Hearn, P. T. Newell, and C.-I. Meng (1995), A satellite study of dayside auroral conjugacy, *Ann. Geophys.*, *13*(11), 1134–1143.

Wei, C. Q., and L. C. Lee (1993), Coupling of magnetopause-boundary layer to the polar ionosphere, *J. Geophys. Res.*, *98*(A4), 5707–5725.

M. O. Fillingim, H. U. Frey, T. J. Immel, S. B. Mende, and G. K. Parks, Space Sciences Laboratory, University of California, 7 Gauss Way, Berkeley, CA 94720, USA. (matt@ssl.berkeley.edu)